Journal of Astronomical Telescopes, Instruments, and Systems

AstronomicalTelescopes.SPIEDigitalLibrary.org

Carbon nanotube optical mirrors

Peter C. Chen
Douglas Rabin

SPIE.

Carbon nanotube optical mirrors

Peter C. Chen[a,b,c,*] and Douglas Rabin[d]
[a]Lightweight Telescopes, Inc., 5469 Hound Hill Court, Columbia, Maryland 21045, United States
[b]Catholic University of America, Institute for Astrophysics and Computational Sciences, 620 Michigan Avenue, N.E., Washington, DC 20064, United States
[c]NASA Goddard Space Flight Center, Solar Physics Laboratory, Mail Code 671, Greenbelt, Maryland 20771, United States
[d]NASA Goddard Space Flight Center, Heliophysics Science Division, Mail Code 670, Greenbelt, Maryland 20771, United States

Abstract. We report the fabrication of imaging quality optical mirrors with smooth surfaces using carbon nanotubes (CNT) embedded in an epoxy matrix. CNT/epoxy is a multifunctional composite material that has sensing capabilities and can be made to incorporate self-actuation. Moreover, as the precursor is a low density liquid, large and lightweight mirrors can be fabricated by processes such as replication, spincasting, and three-dimensional printing. Therefore, the technology holds promise for the development of a new generation of lightweight, compact "smart" telescope mirrors with figure sensing and active or adaptive figure control. We report on measurements made of optical and mechanical characteristics, active optics experiments, and numerical modeling. We discuss possible paths for future development. [DOI: 10.1117/1.JATIS.1.1.014005]

Keywords: carbon nanotube epoxy; smart materials; telescope mirror; space optics; active optics.

Paper 14007 received May 13, 2014; revised manuscript received Oct. 1, 2014; accepted for publication Oct. 7, 2014; published online Nov. 4, 2014.

1 Introduction

Carbon nanotube epoxy (CNT/E) is a member of a new class of multifunctional or "smart" materials. It is a combination of epoxy, a thermoset polymer that features low density and high-dimensional stability, and CNTs, which possess high modulus, high electrical conductivity, high thermal conductivity, large ratio of surface area to mass, piezoresistivity, and an ability to actuate due to electrochemical charge injection and expansion in length of the C—C bond.[1] CNT/E has received much attention as a smart material with many interesting properties.[2,3] One of the material's most intriguing attributes is its ability to sense temperature, strain, and directional deformations.[4] CNTs and CNT/E have also been used to make many types of actuators.[5–7]

If the material can be used to make optical mirrors, CNT/E would be an enabling technology for future telescopes in space and on the ground. Modern large telescopes are based on active optics.[8] In an active system, the primary mirror comprises one or more thin meniscus shells. External sensors and actuators are attached to the back of the mirror to bend or deform the optical surface so as to counteract the effects of gravity, thermal distortion, and wind buffeting. In the case of segmented mirror telescopes such as the Keck Telescope or the James Webb Space Telescope, edge sensors are used to cophase the segments. If CNT/E can be used in place of traditional glass or metal or ceramics, the result would be smart mirrors that have the built-in ability to sense and actuate without the need for external components. This development could lead to substantial reductions in system mass, complexity, power, and cost, as well as increased compactness and reliability.

*Address all correspondence to: Peter C. Chen, E-mail: peter.c.chen@nasa.gov

2 Experimental Procedure

CNT/E mirrors are made by a process of optical replication as shown in Fig. 1.

A glass mandrel is coated with a release agent. A structure of polyurethane rubber is built around the mandrel to hold liquid. Multiwall CNTs mixed with diglycidyl ether of bisphenol-A (DEGBA) and a solvent are subjected to high shear mixing and ultrasonication to de-agglomerate the CNT bundles and form a uniform dispersion. The solvent is evaporated away by heat and vacuum. Next, the curing agent is added and mixed into a slurry. After vacuum degassing, the slurry is poured onto the mandrel and cured in an oven at a moderate temperature for several days. The process is repeated to add more layers behind the optical surface as needed. After the desired number of layers and thicknesses has been achieved, the assembly of mandrel and resin is placed in the oven and postcured. A very slow cool-down ensues followed by an annealing sequence to relieve stress. The entire operation takes place over a period of several weeks. Finally, the assembly is removed from the oven and the replica is released from the mandrel. The replicated mirrors are then measured by interferometry to quantify figure quality and smoothness (root mean square surface microroughness). The same procedure is used to make sets of rectangular bar samples for mechanical characterization.

3 Experimental Results

3.1 *Mechanical Samples*

A number of bar samples $7 \times 2 \times 1$ cm^3 were made. Dynamic elastic properties were measured at room temperature by BuzzMac International LLC of Glendale, Wisconsin, using a proprietary nondestructive impulse excitation test system. Results as provided by the company are given in Tables 1–3.

The sample length was measured with a micrometer of 9.01-mm precision and the width and height to 0.001-mm precision.

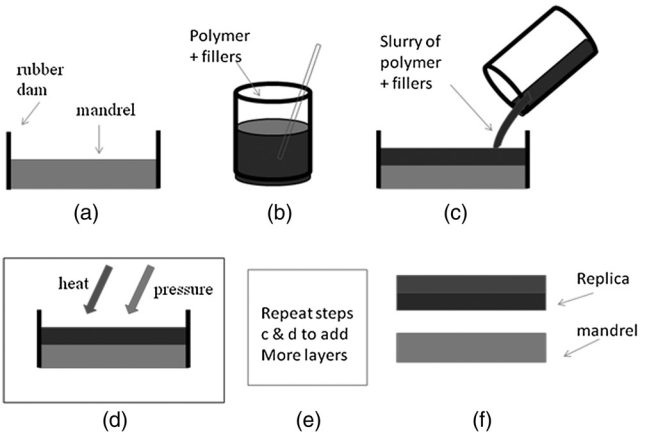

Fig. 1 Fabrication procedure for CNT/E optics. (a) Prepare mandrel. (b) Mix solution. (c) Pour onto mandrel. (d) Cure in oven. (e) Multiple layers. (f) Remove replica.

Table 1 Bar sample bulk properties.

Length (mm)	Width (mm)	Height (mm)	Mass (g)	Density (g cm^{-3})
70.8	19.7	9.7	16.2	1.19

Table 2 Bar sample resonant frequency measurements.

Out-of-plane flexure (Hz)	In-plane flexure (Hz)	Longitudinal (Hz)	Torsional (Hz)
3504	6138	13355	5958

Table 3 Bar sample elastic moduli measurements.

E_{out} (Gpa)	E_{in} (Gpa)	E_l (Gpa)	E_{av} (Gpa)	G (Gpa)	μ_{out}	μ_{in}	μ_l	μ_{av}
4.12	4.17	4.3	4.2	1.55	0.329	0.345	0.385	0.353

Note: E: Young's modulus; G: shear modulus; μ: Poisson ratio.
Subscripts denote mode of vibration.
Out = out-of-plane; in = in-plane; l = longitudinal; av = average.

The mass was measured to 0.01-g precision. The frequencies were measured to 6 Hz or better precision. A total measurement error of ~0.3% is estimated for the Young's modulus derived from the flexural frequency. The tolerances conform to ASTM E1876-09 specifications.

3.2 *Optical Samples*

We made CNT/E optical mirrors in many sizes, shapes, compositions, constructions, and optical functions. Most samples are optical flats, but a number of curved mirrors have also been made in the shape of spheres, parabolas, and hyperbolas. In Fig. 2, there are three samples showing the reflections from a lighted rectangular hole pattern. Here, we present data and discussions on the 5-cm diameter mirror shown in Fig. 1(a) that has the best optical figure obtained to date.

3.2.1 *Optical characterization*

The 5-cm homogeneous CNT/E mirror was measured with a Zygo interferometer. The result is shown in Fig. 3.

3.2.2 *Surface roughness measurements*

The 5-cm replica flat mirror of homogeneous composition was measured at a number of randomly chosen positions using a 4D Technology FizCam 3000 Dynamic Laser Interferometer. The results are listed in Table 4.

3.2.3 *Simple active optics experiment*

A simple experiment was performed to study active figure control. Figure 4(a) is the interferogram obtained by overlaying a 5-cm reference glass flat on top of a 5-cm replica (contact interferometry).[9] A densely packed pattern of curved fringes is seen. The amount of curvature, measured by laying a straight edge across the pattern, is seen to be about three waves at the wavelength of sodium light (589.3 nm). By applying light pressure (estimated force ~3 to 4 N) with a fingertip [shadow at the lower left corner of Fig. 4(b)] the fringes become wider, less numerous, and less curved. By pressing down with the thumb [Fig. 4(c)] with an estimated force of 40 N, the fringes become wide, straight, and parallel. In effect, the application of a light to moderate force in this case sufficed to deform the replica in such a way as to reduce tip/tilt and the spherical aberration (SA) terms. The dark spots seen in the interferograms are caused by micron-sized impurities in the CNT samples.

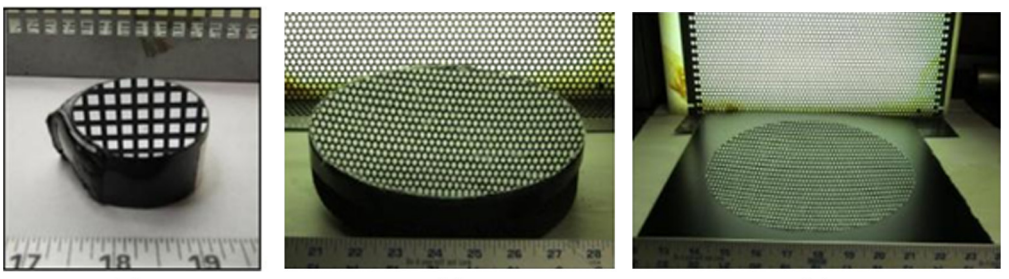

Fig. 2 CNT epoxy nanocomposite mirrors. (a) 5-cm diameter, 1-cm-thick optical flat of homogeneous composition. (b) 20-cm diameter heterogeneous composition mirror with a 3-mm thick facesheet bonded to a 5-cm thick rigid carbon foam backing. (c) Thin (2-mm) facesheet adaptive mirror 25 cm in diameter.

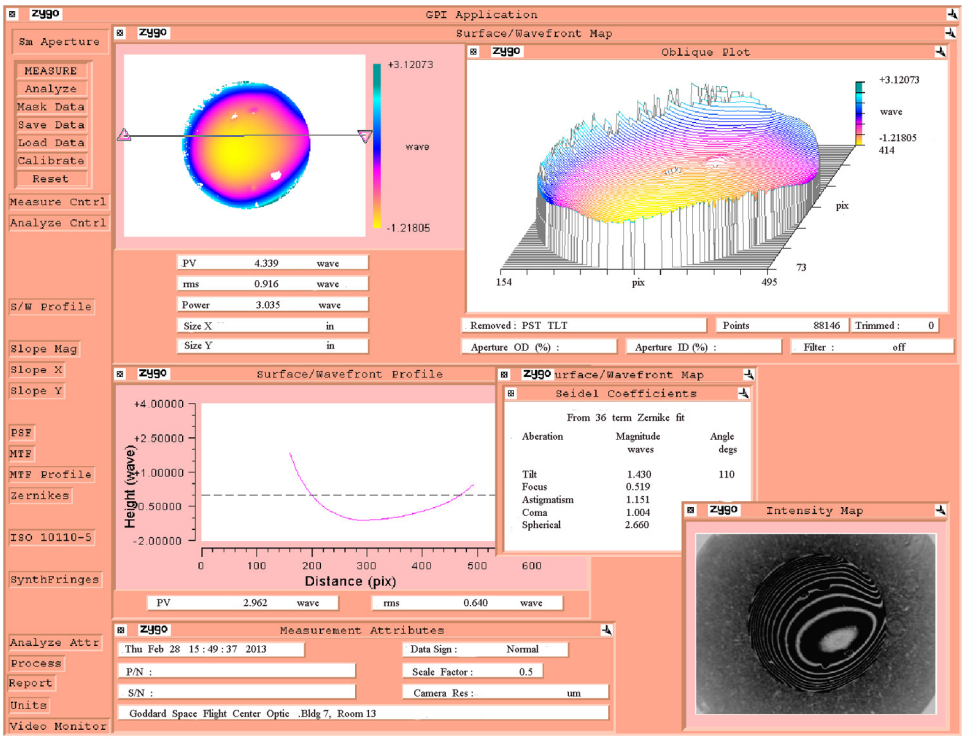

Fig. 3 Zygo interferometer measurement of the 5-cm diameter CNT/E mirror.

Table 4 Surface microroughness measurements.

	Center	Edge 1	Edge 2	Edge 3	Edge 4	Mean
P-V (nm)	117	152	164	97	151	136
RMS (nm)	4.0	3.0	4.8	3.9	2.4	3.6

3.2.4 *Numerical modeling and comparison with experiment*

The active optics experiment reported in Sec. 3.2.3 was simple to perform but, according to at the NASA Goddard Space Flight Center, difficult to model without accurate measurements of the optical surfaces and mechanical parts including imperfections. We, therefore, performed a proof-of-principle experiment as follows:

Another 5-cm CNT/E mirror, in contact with a 4.57-cm diameter optical flat, was observed using Newton interferometry under a low pressure sodium vapor lamp. A metal fixture was machined to have a central opening for the reference flat and a step that contacted the CNT/E sample at its rim in a 2-mm-wide band. Figure 5 is a schematic of the test setup. Figure 6 shows the interference fringe patterns observed with and without the applied ring weight.

The OpenFringe interference fringe reduction program (version 10.4.1) written by Dale Eason[10] was used to compute optical surface maps of the CNT/E mirror with and without the applied loading. The program employed a fast Fourier transform algorithm to generate a map for each surface represented by Zernike polynominals. Subtraction of the two Zernike polynomials (1.468-kg weight—no load) yielded a surface whose cross-sectional profile is shown in Fig. 7. The difference in height of the two surfaces is seen to be ~200 nm.

Next a NASTRAN model was computed using the following parameters: a right cylinder of diameter 5.0 cm, thickness 2.5 cm, Young's modulus 4.2 GPa, and Poisson's ratio 0.353. The top surface is flat. The bottom faces of the cylinder are fixed. A force of 1.5 kg (14.7 N) is applied at the top surface over an annulus 2-mm wide at the rim. The resulting surface is

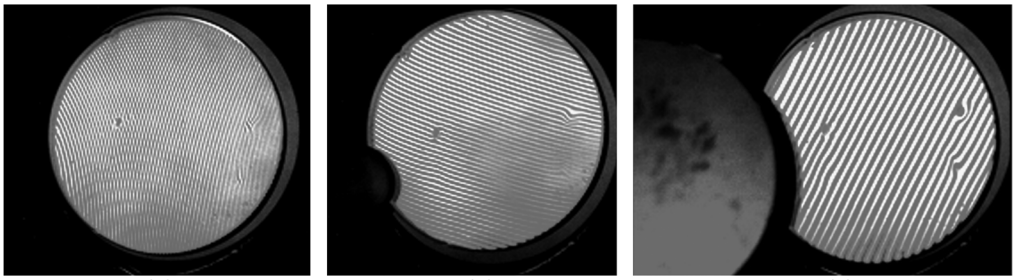

(a) (b) (c)

Fig. 4 The 5-cm diameter replica flat mirror viewed under light from a sodium lamp (589.3 nm) against a reference flat. Dark shadows at lower left corner in frames (b) and (c) are from a thumb pressing down on the reference flat.

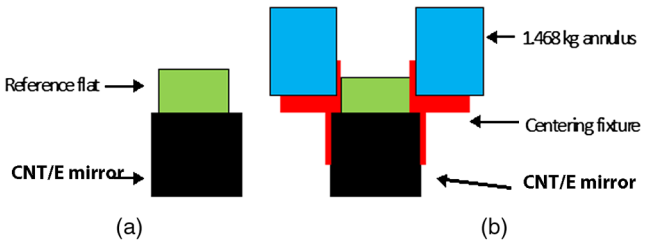

Fig. 5 Schematic of the test apparatus. (a, b) A fixture (red) holds a ring weight (blue) so that the force is applied to the outer rim of the CNT/E mirror (black).

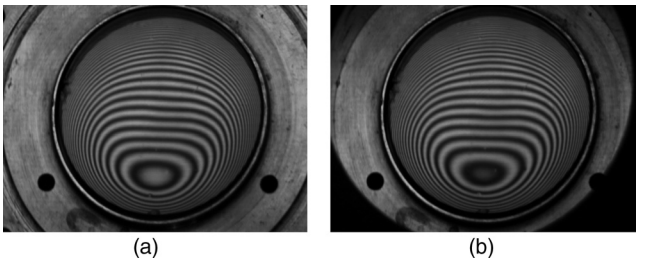

Fig. 6 Interferograms of a 5-cm CNT/E mirror. (a) No weight applied. (b) With a 1.468-kg ring weight.

shown in Fig. 8(a). Figure 8(b) is a cross section taken through the center of the cylinder.

It can be seen from Fig. 8 that the top face of the cylinder, when loaded with a 1.5-kg force at the rim, is changed from a flat surface to a protrusion of height $\sim 10^{-4}$ mm = 100 nm. This is within the same order of magnitude as the measured displacement (Fig. 7). The difference between the observed and the predicted values can most likely be attributed to noise in the numerical fringe reduction process as well as the fact that the CNT/E optic is not a geometrically perfect cylinder.

4 Discussion

4.1 *Mechanical Properties*

The measurements show that CNT/epoxy is a low density material at 1.2 g cm^{-3}. The uniformity in the values of the Poisson ratio and Young's modulus in the three orthogonal directions confirms that the material is homogeneous and isotropic. As a further check, the fundamental resonance frequency F of a uniform solid rectangular rod in the longitudinal direction is[11]

$$F = (1/2L)(E/\rho)^{1/2},$$

where L is the length of the rod, E its Young's modulus, and ρ its density. Substituting the values from Tables 1–3 of $L = 0.0708$ m, $E = 4.2 \times 10^9$ Pa, and $\rho = 1.19 \times 10^3$ kg m^{-3}, we compute that $F = 13455$ Hz.

This is in reasonable agreement with the measured value of 13355 Hz (Table 2). The assumption of a uniform solid is, therefore, justified.

The mechanical properties of CNT/E bear comment. They are quite different from traditional optical materials. Compared to aluminum, for example, the Poisson ratio is about the same, but the Young's modulus is lower by an order of magnitude (4.2 GPa versus 70 GPa).[12] This suggests two possible paths for the development of large telescope mirrors:

a. Increase the stiffness of the material, or
b. Take advantage of the low modulus (entailing low actuation force) material to make optics that can be either active (global figure adjustment, low order Zernike terms) or adaptive (local figure adjustment, higher order Zernike terms).

These topics will be discussed in Sec. 4.4.

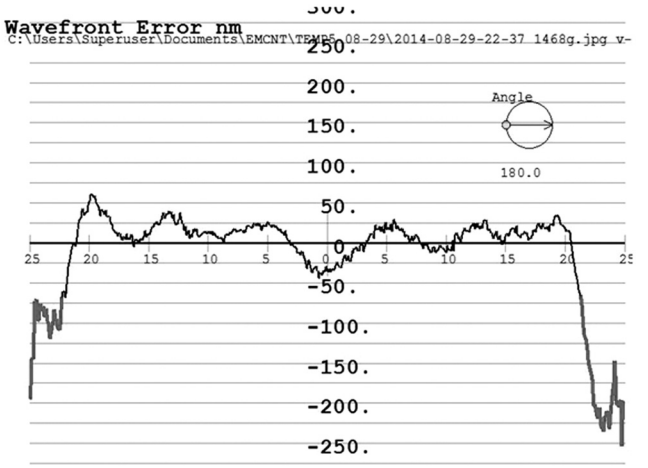

Fig. 7 Cross section of surface formed by subtraction the Zernike polynomials representing the surface of Fig. 6(a) from the corresponding Zernike terms representing the surface of Fig. 6(b).

4.2 *Optical Figure Accuracy*

The interferometric measurement (Fig. 3) shows that the replica deviates from a perfect flat by a peak to valley value of 4.4λ and by rms value of 0.9λ (at 632.8 nm). The corresponding values for the glass mandrel are 0.15λ and 0.01λ, respectively. We note that the largest contribution to the wavefront error is an SA of amplitude $\sim 3\lambda$. Subtracting this term, the residual rms error is reduced to 0.1λ. The presence of the SA term indicates that, despite the care taken in fabrication, there is still much room for improvement. Epoxies shrink as the process of polymerization takes place.[13] Heating, which is required to bring to completion the many chemical reactions inherent in a thermosetting polymer, causes additional cure shrinkage as does the subsequent cool down. The presence of fillers, in this case CNT and other additives, serves to counteract this shrinkage. Therefore, the SA term suggests that there is some amount of residual shrinkage in the replica with respect to the mandrel. The predominance of the SA term is an indication that the shrinkage is largely isotropic; hence confirming again that the material has good uniformity. Overall, the results thus far are encouraging. Work is currently under way to refine the replication procedure toward the goal of fabricating higher quality optics.

4.3 *Surface Smoothness*

The surface rms microroughness is a measure of the surface texture at high spatial frequencies (nanometers to millimeters). This parameter quantifies the ability of an optical system to resolve point sources that are closely spaced.[14] From Table 4, the average value measured at six points on the CNT/E mirror is about 36 Å. The averaged value of six points measured at random on the glass mandrel is 6.0 Å. The difference suggests either that,

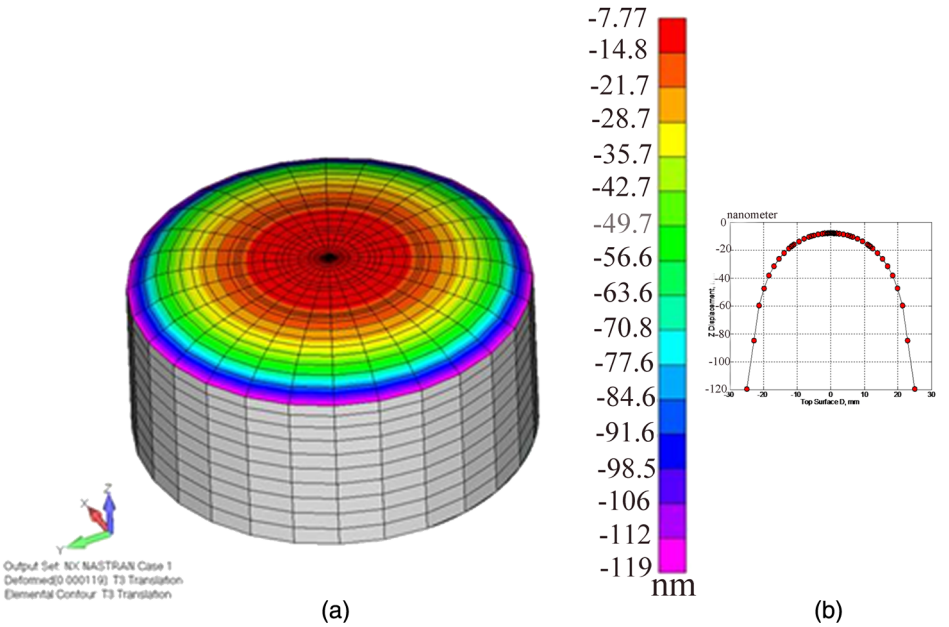

Fig. 8 NASTRAN model computed to show the change in shape of a 5-cm diameter, 2.5-cm-thick CNT/E right cylinder with load applied around its top rim. (a) Solid model and (b) cross section of cylinder through the center. Computations by Babak Farrokh, NASA Goddard Space Flight Center Structural Mechanics Branch.

again, the fabrication process needs improvement, or else the presence of CNTs contributes to the increase in surface roughness. Work is currently under way to produce highly smooth (<10-Å rms) surfaces. We note, however, that the 36-Å value is in the mid-range for polished glass surfaces.[14] Thus CNT/E in its present state appears to be sufficiently smooth for most telescopic applications.

4.4 *CNT/E as an Optical Material*

It remains to be demonstrated that meter-class telescope mirrors can be achieved using this new material. However, on the basis of what is known so far, two statements can reasonably be made:

1. CNT mirrors can be fabricated by replication[15] and by spincasting. Spincast epoxy mirrors without CNTs have been made and used successfully by Neugebauer and Leighton,[16] and parabolas as large as 10 m have been made.[17] Moreover, since the precursor material is a liquid slurry, CNT/E can be dispensed through the nozzle of a three-dimensional (3-D) printer. This procedure may enable the fabrication of athermal telescope systems where both the optics and structures are made from the same material. In principle, it is possible to employ 3-D printing to fabricate optical mirrors as well to near net shape, to be followed by some form of post figuring. This possibility remains to be investigated.

2. The multilayer construction, plus the ability to change the composition and thickness of each layer, permits an almost infinite number of configurations. Suppose it is desired to increase the stiffness of the mirror substrate, one can, for example, employ single wall CNTs,[18] vary the diameter and length/diameter ratio of the CNTs, functionalize the nanotubes to enhance bonding to the matrix, use special processing procedures and/or coupling agents, or incorporate micro- or macrosize fillers to make multiscale composite structures.[19,20]

4.5 *Implementing Active Optics*

The simple experiment described in Fig. 3 above illustrates the ease with which the optical surface can be adjusted. It suggests that active figure control in CNT/E mirrors would not require high force, high power, and relatively massive actuators typical of other mirror technologies. In fact, with the appropriate construction, external components may not be required at all.

An active optics system requires the ability to sense and to actuate. For CNT/E, the sensing function can be built-in. Temperature and strain can be monitored by measuring the resistance at various points in the substrate without the use of external sensors.[4] Actuation can be effected by heat, taking advantage of the ability of CNT/E to function as a heating element.[21] Alternatively, specifically designed actuation layers can be added into the substrate. Such a layer can contain, for example, embedded shape memory alloy wires,[22,23] CNTs aligned by mechanical, electrical, or magnetic means,[24] CNT yarns,[25] or piezoelectric powders.[26,27]

In summary, CNT/E as it exists is a low density material capable of giving a 1λ rms optical figure and 40-Å rms surface microroughness. The uniformity of the measured resonance frequencies in the three orthogonal directions, and the good agreement between observed and computed values, show that the material is homogeneous and isotropic. The relatively low modulus of elasticity (compared to traditional optical materials) suggests that active figure control in CNT/E can be accomplished with low force requirements. This is confirmed by a simple experiment using manual actuation. There appear to be numerous ways to implement self-sensing functions and embedded actuators into the mirror substrate. These remain to be explored.

5 Conclusion

We have shown that it is possible to make imaging quality mirror surfaces based on CNT epoxy composites. The material is homogeneous and isotropic and has a low density. The low modulus of elasticity shows that active figure control can be accomplished with low force and hence low-power actuators. An experiment to study the deformation of an optical surface under an applied load showed reasonable agreement between the observed and predicated values. CNT/E is, therefore, a promising technology for making lightweight, ultracompact active telescope mirrors with embedded sensing and actuation. Since the fabrication starts with a liquid slurry, novel processes of making telescope mirrors become possible, including optical replication, spincasting, and 3-D printing. The result is preliminary, however. Much work remains to be done to verify the feasibility of making larger optics and to study various factors such as the long-term dimensional stability of coated mirror surfaces in Earth environment (for ground applications) and under cryogenic vacuum conditions (for space telescopes).

Acknowledgments

We thank P. Mirel, P. Cursey, M. Perry, and M. Saulino (NASA GSFC) for helpful advice and discussions. C. Strojny (NASA GSFC Optics Branch) made the surface roughness measurements. B. Farrokh (NASA GSFC Structural Mechanics Branch) performed the NASTRAN modeling. Mechanical measurements were made by P. Bosomworth (Buzzmac Co.). We thank Dale Eason for advice with the OpenFringe interference fringe reduction program. We thank R. Stesky and C. Stesky for editorial advice. This work was supported in part by NASA Co-Operative Agreement #NNG11PL10A with the Catholic University of America.

References

1. S. B. Jain et al., "Building smart materials based on carbon nanotubes," *Proc. SPIE* **5389**, 167–175 (2004).
2. I. Kang et al., "Introduction to carbon nanotube and nanofiber smart materials," *Composites: Part B* **37**, 382–394 (2006).
3. K.-T. Lau and D. Hui, "The revolutionary creation of new advanced materials—carbon nanotube composites," *Composites: Part B* **33**, 263–277 (2002).
4. W. M. Wichmann et al., "Direction sensitive bending sensors based on multi-wall carbon nanotube/epoxy nanocomposites," *Nanotechnology* **19**, 475503 (2008).
5. Y.-H. Yun et al., "Development of novel single-wall carbon nanotube-epoxy composite ply actuators," *Smart Mater. Struct.* **14**, 1526–1532 (2005).
6. Y. Wei et al., "Thermoacoustic chips with carbon nanotube thin yarn arrays," *Nano Lett.* **13**(10), 4795–4801 (2013).
7. M. Lima et al., "Electrically, chemically, and photonically powered torsional and tensile actuation of hybrid carbon nanotube yarn muscle," *Science* **338**(6109), 928–932 (2012).
8. R. N. Wilson, "Modern telescope developments: pupil segmentation and techniques to reduce mass," *Reflecting Telescope Optics II* (Ch. 3), pp. 169–348, Springer, New York (1999).
9. M. V. Mantravadi, "Newton, Fizeau, and Haidinger interferometers," *Optical Shop Testing*, 2nd ed., D. Malacara, Ed., pp. 1–49, John Wiley & Sons, New York (1999).
10. D. Eason "OpenFringe Interferogram Mirror Analysis Openfringe 10," http://openfringe.sourceforge.net, see also, https://groups.yahoo.com.neo/groups/interferometry/files/OpenFringe Beta/ (19 October 2014).
11. H. J. McSkimin, "Theoretical analysis of modes of vibration for isotropic rectangular plates having all surfaces free," *Bell Labs Tech. J.* **23** (Ch. 8), 151–177 (1944).
12. R. N. Wilson, "Modern telescope developments: pupil segmentation and techniques to reduce mass," *Reflecting Telescope Optics II* (Ch. 3), pp. 220–221, Springer, New York (1999).
13. L. S. Penn and H. Wang, "Epoxy resins," *Handbook of Composites*, 2nd ed., S. T. Peters, Ed., pp. 48–74, Chapman and Hall, London, UK (1988).
14. H. E. Bennett, "Optical microroughness and light scattering in mirrors," *Encyclopedia of Optical Engineering*, Vol. 2, R. G. Driggers et al., Eds., pp. 1730–1737, CRC Press, Boca Raton, Florida (2003).
15. H. Wahl, "Light-weight replicated optics," *Proc. SPIE* **0115**, 34–39 (1977).
16. M. Harwit, "Neugebauer, Martz, and Leighton's observations of extremely cool stars," *ApJ*, Centennial Issue **525C**, 1063–1064 (1999).
17. F. J. Schmidt, "Electroforming of large mirrors," *Appl. Opt.* **5**(5), 719–725 (1966).
18. X. Li et al., "Nanomechanical characterization of single-walled carbon nanotube reinforced epoxy composites," *Nanotechnology* **15**, 1416–1423 (2004).
19. J. Qiu et al., "Carbon nanotube integrated multifunctional multiscale composites," *Nanotechnology* **18**, 275708 (2007).
20. T. Filleter and H. D. Espinosa, "Multi-scale mechanical improvement produced in carbon nanotube fibers by irradiation cross-linking," *Carbon* **56**, 1–11 (2013).
21. H. C. Neitzert, L. Vertuccio, and A. Sorrentino, "Epoxy/MWCNT composite as temperature sensor and electrical heating element," *IEEE Trans. Nanotech.* **10**(4), 688–693 (2011).
22. J. A. Balta et al., "Smart composites with embedded shape memory alloy actuators and fibre Bragg grating sensors: activation and control," *Smart Mater. Struct.* **14**, 457–465 (2005).
23. E. L. Kirkby et al., "Tailored processing of epoxy with embedded shape memory alloy wires," *Smart Mater. Struct.* **18**, 095043 (2009).
24. S.-H. Hwang et al., "Smart Materials and Structures Based on Carbon Nanotube Composites," *Carbon Nanotubes—Synthesis, Characterization, Applications*, S. Yellampalli, Ed., InTech, Rijeka, Croatia (2011).
25. C. Li, E. T. Thostenson, and T.-W. Chou, "Sensors and actuators based on carbon nanotubes and their composites: a review," *Compos. Sci. Technol.* **68**, 1227–1249 (2008).
26. S. Tian, F. Cui, and X. Wong "New type of piezo-damping epoxy-matrix composites with multi-wall carbon nanotubes and lead zirconate titanate," *Mater. Lett.* **62**, 3859–3861 (2008).
27. M. C. Ray and R. C. Batra, "Effective properties of carbon nanotube and piezoelectric fiber reinforced hybrid smart composites," *J. Appl. Mech.* **76**(3), 034503 (2009).

Peter C. Chen is president of Lightweight Telescopes, Inc. and research astrophysicist at the NASA Goddard Space Flight Center. He received a BSc in physics (University of Toronto) and a PhD in astronomy (Case Western Reserve University). He has worked in the fields of stellar polarimetry, lunar occultation, space ultraviolet telescope optics and instrumentation, and high temperature superconductor bearings. His current interests are composite and nanocomposite optics, moondust telescopes, and extremely low reflectance carbon nanotube coatings.

Douglas Rabin is a research astrophysicist at NASA Goddard Space Flight Center. He received his AB in astronomy from Harvard College and his PhD in astronomy from the California Institute of Technology. His research interests include the structure and dynamics of the solar corona and astronomical instrumentation.